High resolution Brillouin scattering studies of β-$Gd_2(MoO_4)_3$; the bulk and surface phase transitions

2005 J. Phys.: Condens. Matter 17 587

(http://iopscience.iop.org/0953-8984/17/4/003)

INSTITUTE OF PHYSICS PUBLISHING JOURNAL OF PHYSICS: CONDENSED MATTER

J. Phys.: Condens. Matter **17** (2005) 587–598 doi:10.1088/0953-8984/17/4/003

High resolution Brillouin scattering studies of β-$Gd_2(MoO_4)_3$; the bulk and surface phase transitions

S Mielcarek[1], A Trzaskowska[1], B Mroz[1] and T Andrews[2]

[1] Faculty of Physics, Adam Mickiewicz University, Umultowska 85, 61-614 Poznan, Poland
[2] Department of Physics and Oceanography, Memorial University of Newfoundland, St John's, Newfoundland, A1B 3X7, Canada

Received 10 September 2004, in final form 17 November 2004
Published 14 January 2005
Online at stacks.iop.org/JPhysCM/17/587

Abstract

We present here results of Brillouin scattering from bulk and surface phonons propagating in a well known ferroelectric–ferroelastic crystal β-$Gd_2(MoO_4)_3$, in the temperature range covering the phase transition. Temperature dependences of the velocity of Rayleigh surface acoustic waves, propagating in a few planes of this crystal, have been calculated. The surface phonon velocities determined experimentally have been found to show a different character of temperature dependences, especially in the phase transition range.

1. Introduction

For the last ten years significant attention has been paid to the physics of real surfaces of different solids in terms of their elastic properties and phonon dynamics. Different experimental methods have been used, covering a wide range of surface and near surface layers, ranging from one layer of surface atoms in the method of helium scattering, through the electron beam scattering seeing only a few layers to the quasi-surface investigation with the use of ultrasonic methods working in the micrometric scale. Development of high resolution Brillouin spectroscopy, based on tandem Fabry–Perot spectrometers, has facilitated investigation of surface phonons of wavelength of hundreds of nanometres matching the sizes of different interesting objects, for example the so-called brushes of porous silicon [1], nanolayers of metals or regular arrays of Ni nanoislands.

The elastic properties of real solid surfaces have been intensely studied recently in view of the high and specific demands of new technologies [2, 3]. In non-transparent solids the phonons observed in the Brillouin spectrum are related exclusively to their surface since the scattering volume lies very close to the surface. In the Brillouin spectra of transparent solids the bulk phonons dominate and observation of surface phonons is difficult because of a small surface reflection coefficient. However, it has been established that a thin metallic film covering the surface and enhancing the surface reflection coefficient has no effect on the spectrum of surface phonons [3–6]. The thin metallic film $h < 60$ nm permits the observation of the Rayleigh surface acoustic waves (Rayleigh SAWs) in the substrate. For the films of greater thickness pseudo-SAWs are observed that interact with the substrate vibrations. For still thicker metal

films we observe the Rayleigh waves propagating in the deposited film. Generally, for the last 20 years this method has been mostly applied to opaque materials for which the observation of surface phonon spectra is fast and easy [2, 7].

This paper presents the results of a study of Rayleigh SAWs propagating in the near surface layers of the ferroelectric–ferroelastic crystal β-$Gd_2(MoO_4)_3$ (β-GMO). The motivation of our studies follows from the interesting elastic properties of such materials; the ferroelastics show critical temperature behaviour of some of their elastic constants at the phase transition. When analysing the properties of surface acoustic waves, it is obvious that in the ferroelastic material their velocities around T_C must be related to the velocity of the so-called soft mode [8]. Knowing the bulk elastic properties it is easy to predict the temperature behaviour of the velocity of the surface phonon and then of course it is natural to compare the calculated results with the value of v_R obtained directly from a high resolution Brillouin experiment. This is the main aim of the paper presented.

2. The crystal and the apparatus

The β-GMO crystal undergoes the ferroelectric–ferroelastic phase transition from the tetragonal point group $\bar{4}2m$ to the orthorhombic $mm2$ at about 430 K [9]. The thermodynamical theory describing the phase transition in this crystal has been proposed by Dvorak [10], who assumed a two-component order parameter to account for the spontaneous polarization and spontaneous deformation occurring in the crystal. The elastic properties of the β-GMO crystal have been studied by the ultrasonic method [11], piezoelectric resonance [12] and Brillouin spectroscopy [13–15]. The available literature data provide information on the temperature dependences of the c_{11} and c_{22} elastic constants [14], while the other components were determined only at 293 and 473 K [13].

The β-GMO crystals with the melting point temperature of 1430 K were obtained by the Czochralski method. The crystals were grown from stoichiometric solutions in an iridium crucible in argon atmosphere. The typical size of the colourless crystals of good optical quality is a few cubic centimetres and their density is $\rho = 4.565$ g cm^{-3}. The crystals show two cleavage planes perpendicular to the [001] and [100] directions. Samples of several different orientations for the purpose of Brillouin scattering were prepared in the shape of rectangles of edge length of a few millimetres. The observation and analysis of the scattered light was performed using a Brillouin spectrometer working in a tandem system (JRS Scientific Instruments) [7]. The experimental set-up applied, permitting a simultaneous realization of two scattering geometries of 90° and 180°, was described in detail in our earlier work [16].

The light source was an Nd:YAG single-mode diode-pumped laser of power 200 mW, emitting the second harmonic of the length $\lambda = 532$ nm (Coherent Laser Group, model 532). The samples were mounted in a high temperature holder. The temperature was stabilized within ± 0.1 K.

The refraction indices in particular directions along which the elastic properties were studied, for $\lambda = 532$ nm, were $n_x = 1.8529$, $n_y = 1.8533$ and $n_z = 1.909$ at room temperature and $n_x = n_y = 1.853$ and $n_z = 1.929$ in the tetragonal phase [13, 17].

The bulk phonon velocity v_B can be calculated from the equation

$$v_B = \frac{\lambda \Delta \nu_B}{\sqrt{n_i^2 + n_s^2 - 2n_i n_s \cos\beta}} \tag{1}$$

where $\Delta\nu_B$ is the frequency shift determined from the Brillouin scattering spectra, n_i and n_s are the refraction indices along the directions of incident (i) and scattered (s) light and β is the scattering angle [18].

Table 1. ρv^2 as a function of the elastic constants in the tetragonal $\bar{4}2m$ and orthorhombic $mm2$ phases.

Phonon		Modes	Tetragonal phase $\bar{4}2m$	Orthorhombic phase $mm2$
[100]	γ_1	L	c_{11}	c_{11}
	γ_2	T_1	c_{66}	c_{66}
	γ_3	T_2	c_{44}	c_{55}
[010]	γ_4	L	c_{11}	c_{22}
	γ_5	T_1	c_{44}	c_{44}
	γ_6	T_2	c_{66}	c_{66}
[001]	γ_7	L	c_{33}	c_{33}
	γ_8	T_1	c_{44}	c_{55}
	γ_9	T_2	c_{44}	c_{44}
[110]	γ_{10}	L	$\frac{1}{2}[(c_{11}+c_{66})+(c_{12}+c_{66})]$	$\frac{1}{4}[(c_{11}+c_{22}+2c_{66}) + \sqrt{(c_{11}-c_{22})^2+4(c_{12}+c_{66})^2}]$
	γ_{11}	T_1	$\frac{1}{2}[(c_{11}+c_{66})-(c_{12}+c_{66})]$	$\frac{1}{4}[(c_{11}+c_{22}+2c_{66}) - \sqrt{(c_{11}-c_{22})^2+4(c_{12}+c_{66})^2}]$
	γ_{12}	T_2	c_{44}	$\frac{1}{2}(c_{55}+c_{44})$
[101]	γ_{13}	L	$\frac{1}{4}[(c_{11}+c_{33}+2c_{44}) + \sqrt{(c_{11}-c_{33})^2+4(c_{13}+c_{44})^2}]$	$\frac{1}{4}[(c_{11}+c_{33}+2c_{55}) + \sqrt{(c_{11}-c_{33})^2+4(c_{13}+c_{55})^2}]$
	γ_{14}	T_1	$\frac{1}{4}[(c_{11}+c_{33}+2c_{44}) - \sqrt{(c_{11}-c_{33})^2+4(c_{13}+c_{44})^2}]$	$\frac{1}{4}[(c_{11}+c_{33}+2c_{55}) - \sqrt{(c_{11}-c_{33})^2+4(c_{13}+c_{55})^2}]$
	γ_{15}	T_2	$\frac{1}{2}(c_{66}+c_{44})$	$\frac{1}{2}(c_{66}+c_{44})$
[011]	γ_{16}	L	$\frac{1}{4}[(c_{11}+c_{33}+2c_{44}) + \sqrt{(c_{11}-c_{33})^2+4(c_{13}+c_{44})^2}]$	$\frac{1}{4}[(c_{22}+c_{33}+2c_{44}) + \sqrt{(c_{22}-c_{33})^2+4(c_{23}+c_{44})^2}]$
	γ_{17}	T_1	$\frac{1}{4}[(c_{11}+c_{33}+2c_{44}) - \sqrt{(c_{11}-c_{33})^2+4(c_{13}+c_{44})^2}]$	$\frac{1}{4}[(c_{22}+c_{33}+2c_{44}) - \sqrt{(c_{22}-c_{33})^2+4(c_{23}+c_{44})^2}]$
	γ_{18}	T_2	$\frac{1}{2}(c_{66}+c_{44})$	$\frac{1}{2}(c_{66}+c_{55})$

The elastic constants c_{ijkl} were determined from the Christoffel equation (2) [19]:

$$|c_{ijkl}q_jq_k - \rho v^2\delta_{il}| = 0 \tag{2}$$

where q_j, q_k are the direction cosines, ρ the crystal density and c_{ijkl} the elasticity tensor.

In the prototype phase the elastic properties of the β-GMO crystal are described by the six independent elastic constants, c_{11}, c_{33}, c_{44}, c_{66}, c_{12} and c_{13}; in the ferroelastic phase the number of independent components increases to nine: c_{11}, c_{22}, c_{33}, c_{44}, c_{55}, c_{66}, c_{12}, c_{13} and c_{23}. In table 1 we have collected the expressions of ρv^2 as a function of the elastic constants for the tetragonal $\bar{4}2m$ and orthorhombic $mm2$ point groups. It should be noted that in the orthorhombic system the x and y axes of β-GMO are rotated by 45° about the z axis with respect to their orientation in the tetragonal phase. Consequently, the [100] phonon in the $mm2$ phase becomes the [110] phonon in the $\bar{4}2m$ phase.

From the theory of surface acoustic waves [19] it follows that the surface phonon velocity v_R must be lower than that of the slowest transverse bulk phonon:

$$v_R < v_T \tag{3}$$

—the surface phonon velocity v_R is also a linear function of the Brillouin shift,

$$v_R = \frac{\lambda \Delta \nu_R}{2\sin\theta} \tag{4}$$

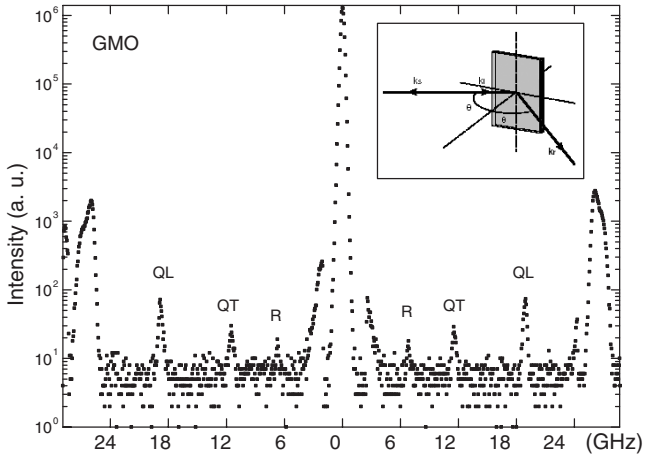

Figure 1. Surface Brillouin spectrum showing the surface (R), quasi-longitudinal (QL) and quasi-transverse (QT) phonons of the β-GMO crystal at room temperature; the inset shows the surface scattering geometry applied.

and may be determined from the slope of the $\Delta\nu_R(2\sin\theta)$ function. In equation (4) θ is the angle of light incidence.

Figure 1 presents a typical example of the surface Brillouin spectrum showing surface (R), quasi-longitudinal (QL) and quasi-transverse (QT) phonons at room temperature. The inset shows the surface scattering geometry applied; k_R is the wavevector of the surface phonon.

3. Results and discussion

3.1. Bulk elastic constants of β-GMO

The temperature dependences of the elastic constants c_{ii} ($i = 1, \ldots, 6$) determined from direct measurements of the Brillouin frequency shift.

Figure 2 presents the temperature dependences of the longitudinal elastic constants c_{11}, c_{22} and c_{33}. The components c_{11} and c_{22} show the same very strong softening when approaching T_C from above. The elastic constant c_{33} was found to be slightly affected by the ferroelastic phase transition.

The temperature dependences of the shear elastic constants c_{44}, c_{55} and c_{66} are given in figure 3. The c_{66} elastic constant is strongly affected by the transition, while the component c_{44} remains almost unchanged in the whole temperature range studied. The components c_{44} and c_{55} take the same value in the prototype and ferroelastic phase. A detailed analysis of the experimental errors in surface Brillouin scattering measurements has been presented in [20]. The authors of this reference have estimated that at the angle of light incidence θ_i of 70° the experimental error is $\pm 0.5\%$. The maximum error in our experiment does not exceed 0.5% of the measured value either.

In order to explain certain controversies in the mode assignment in the [100] direction, figure 4 presents the temperature evolution of the Brillouin spectra. In figure 4(a), showing the spectrum taken at room temperature, there are two clearly marked components of frequencies 18 and 20 GHz, respectively. In terms of the convention developed in the 1970s, assuming the cleavage planes in the β-GMO crystal as perpendicular to the [110] and [001] directions, the

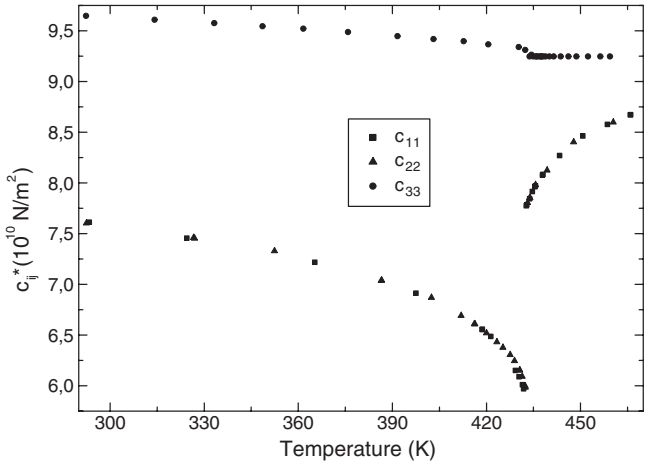

Figure 2. Temperature dependences of the c_{11}, c_{22} and c_{33} elastic constants of the β-GMO crystal.

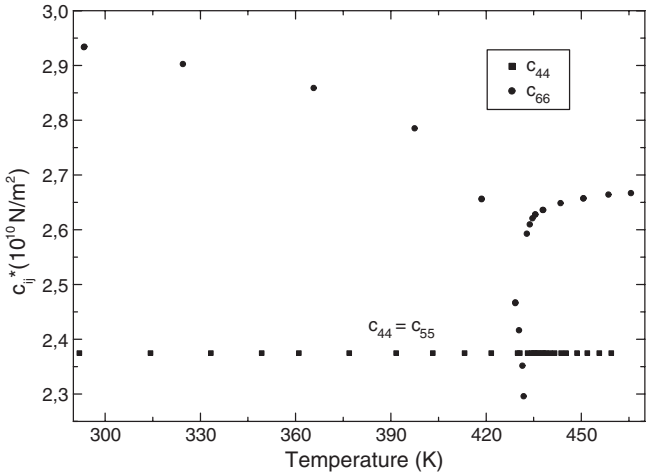

Figure 3. Temperature dependences of the c_{44}, c_{55} and c_{66} elastic constants of the β-GMO crystal.

two components from figure 4 are assigned to the elastic constants c_{11} and c_{66}. This character of the temperature dependence of the phonon frequency in the [100] direction is consistent with the Landau model of ferroelastic phase transition, according to which, for the $\bar{4}2m \rightarrow mm2$ phase transition, a critical behaviour of strain may be expected for the e_6 component [21]. This in turn indicates c_{66} as the most temperature dependent elastic constant.

The non-diagonal components of the elastic constants c_{12}, c_{13} and c_{23} were determined from the temperature dependences of the ρv^2 of γ_{10}, γ_{11}, γ_{13}, γ_{14}, γ_{16} and γ_{17} modes (see table 1). The temperature dependences of the Brillouin frequency shift for the LA phonons propagating along the [110], [101] and [011] directions are given in figure 5. The calculated temperature dependences of c_{12}, c_{13} and c_{23} components are given in figure 6.

The proper values of the elastic constants were found imposing the requirement that the elastic energy must be positive, which for the tetragonal system takes the form [22]

$$c_{11} > |c_{12}|, \qquad (c_{11} + c_{12})c_{33} > 2c_{13}^2, \qquad c_{44} > 0 \qquad \text{and} \qquad c_{66} > 0.$$

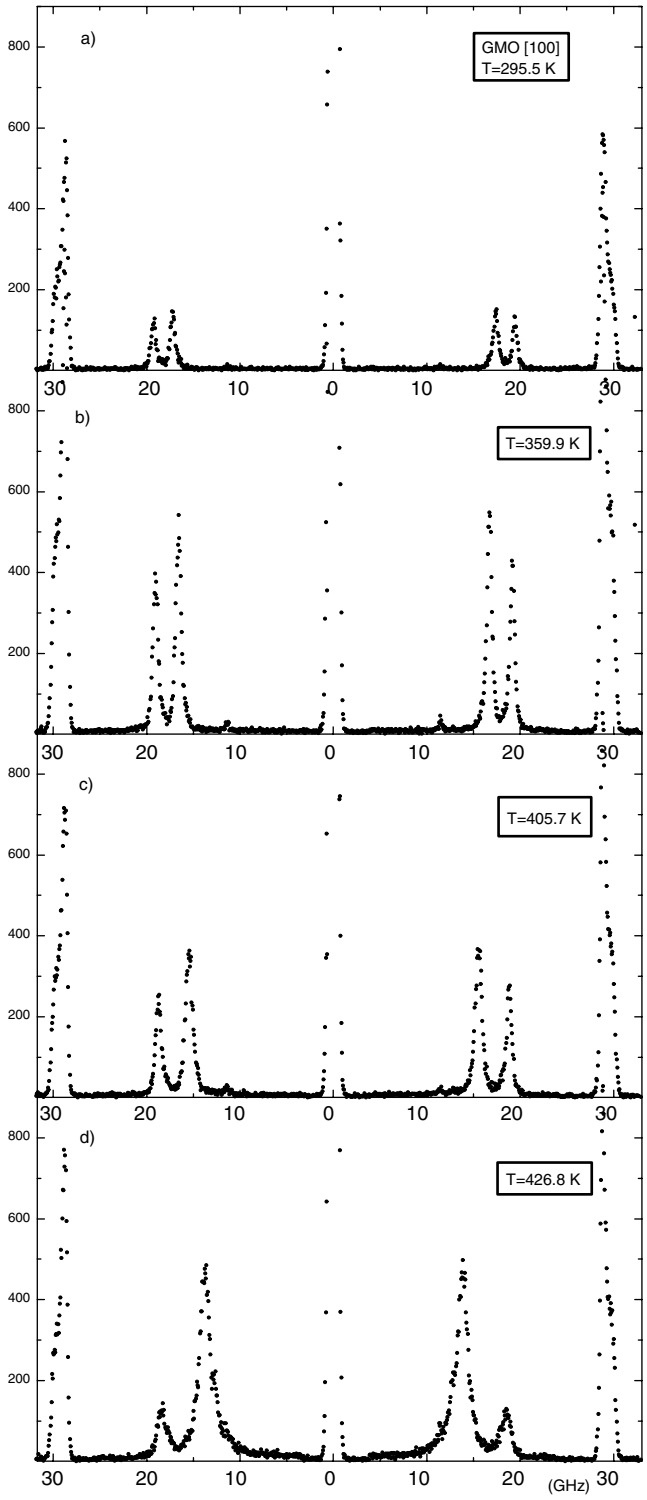

Figure 4. Temperature evolution of the Brillouin spectra of bulk phonons observed in the [100] direction.

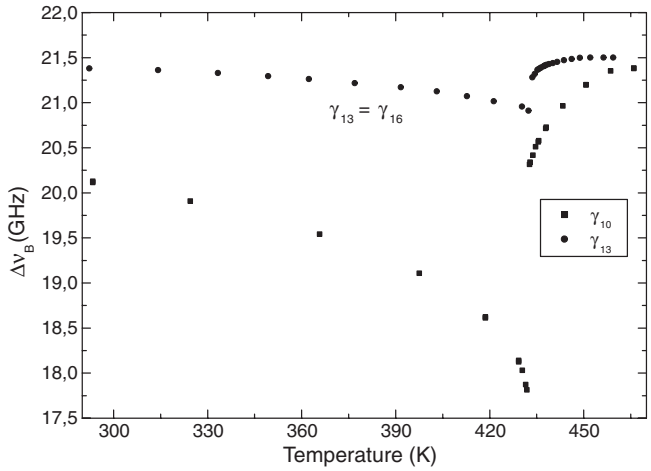

Figure 5. Temperature dependence of the Brillouin frequency shift for the phonons propagating along the [110], [101] and [011] directions (see table 1).

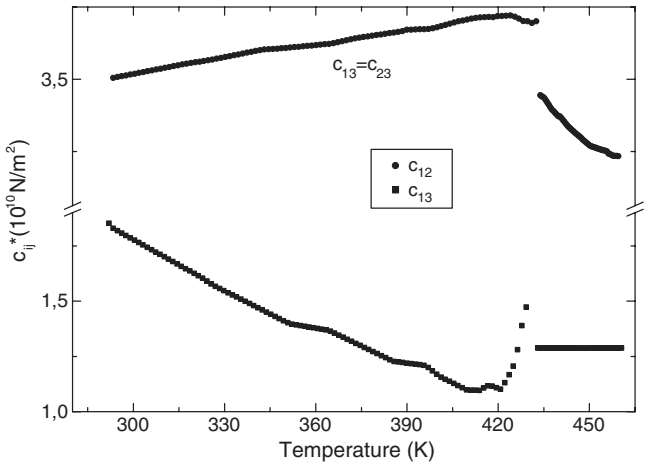

Figure 6. Temperature dependence of elastic constants c_{12}, c_{13} and c_{23}.

As the mixed components of the tensor c_{ij} are not determined directly but can be calculated from a composition of two types of variations LA and TA (e.g. γ_{10} and γ_{11} gives the component c_{12}), the above relation verifies the correctness of the calculations of c_{ij}. The above relation also permits verification of the assignments of the vibrations to the modes.

3.2. The surface phonon velocity calculated from the bulk elastic constants

The surface phonon velocity is determined on the basis of the known bulk elastic constants. For isotropic media the surface wave velocity can be—under some approximations—found from the following equation [19]:

$$v_R \cong v_T \frac{0.87c_{11} + 2c_{12}}{c_{11} + 2c_{12}}. \tag{5}$$

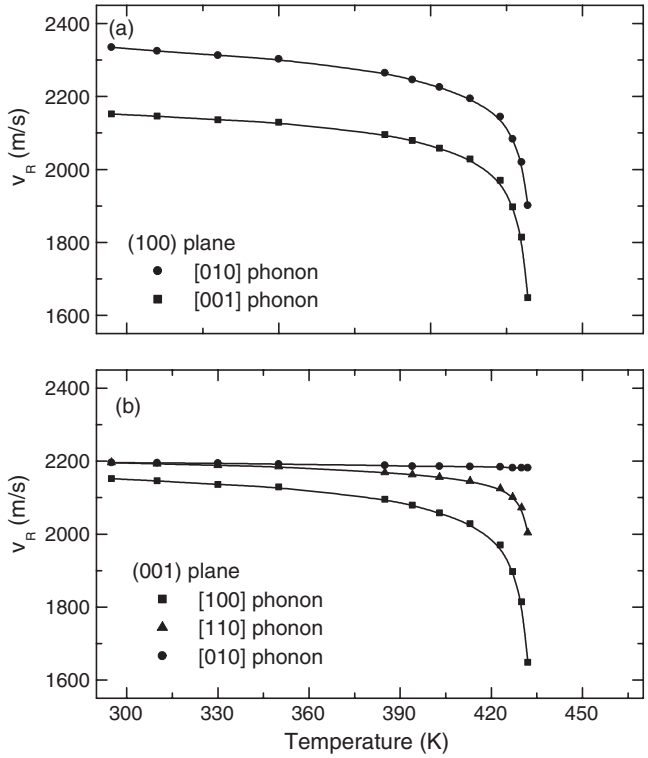

Figure 7. Calculated surface phonon velocities versus temperature in the (100) and (001) planes.

For anisotropic media the Rayleigh surface acoustic wave velocity is determined by the iterative methods, allowing a determination of the surface wave displacement at specific boundary conditions and for a certain crystal symmetry. The fundamental condition for the correct calculations is that the free plane in which the wave propagation is studied must be the symmetry plane of the crystal studied [19]. A typical dependence of the velocity of the Rayleigh SAW versus temperature is shown in figure 7. The calculated temperature dependences of surface phonons in the main planes of the β-GMO crystal reveal a behaviour similar to that of the bulk modes. In contrast to our results presented in the next section, such a behaviour has been experimentally confirmed for the $SrTiO_3$ crystal by ultrasonic measurements using frequencies of the order of 10 MHz corresponding to the surface layer thickness of hundreds of micrometres [23]. With the Brillouin experiment we explore a layer of hundreds of nanometres only.

3.3. Experimental determination of the surface phonon velocity

Our experimental set-up offers a possibility of surface phonon observation at the phase transition. As the β-GMO is transparent it was necessary to bring the scattering volume closer to the surface by coating the samples with a thin Al film (not thicker than 40 nm) [3]. A preliminary study of the surface phonon behaviour on as-cleft planes and on the same planes after their polishing was made. The character of the temperature dependences of the surface phonons has been found to be the same for the samples of these two types, although the samples with the polished planes are characterized by greater active surface. Some selected temperature dependences of the surface phonons in the main crystallographic

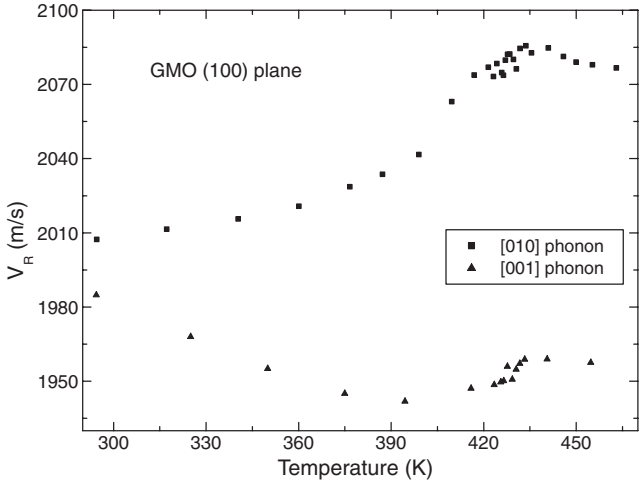

Figure 8. Surface phonon velocities versus temperature—experimental results in the (100) plane.

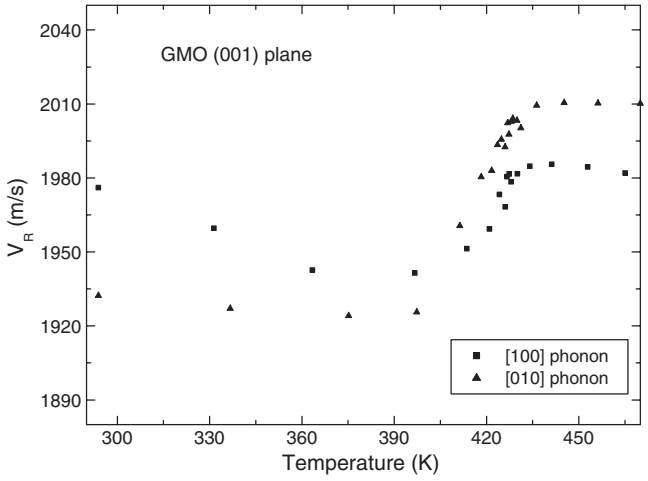

Figure 9. Surface phonon velocities versus temperature—experimental results in the (001) plane.

planes are presented in figures 8–10; the angle of light incidence is $\theta = 60°$. This value of the angle of light incidence provides us with a possibility of observing the behaviour of the surface phonons in a layer of about 300 nm in thickness, propagating in the crystal of β-GMO. Each of the surface phonons revealed anomalous behaviour at the phase transition. The observed anomalies were found to be significantly different from those obtained from the calculations. No surface phonon softening, typical of ferroelastic crystals, was noted. A relatively small jumpwise change in the surface acoustic wave velocity was observed at about T_C (about 50–100 m s^{-1}). The behaviour of the surface phonons in the (100) and (001) planes (see figures 8 and 9) was similar—that is, the phonon velocity increased. In the (010) plane the phonon velocity anomaly was very different (see figure 10), as a distinct maximum of its velocity was observed at T_C.

The configuration of the experimental system permitted a simultaneous observation of the surface and bulk phonons in the whole temperature range studied. Such a simultaneous obser-

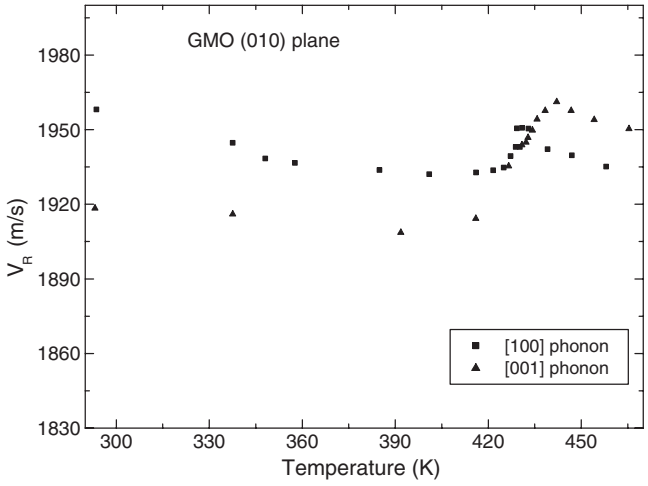

Figure 10. Surface phonon velocities versus temperature—experimental results in the (010) plane.

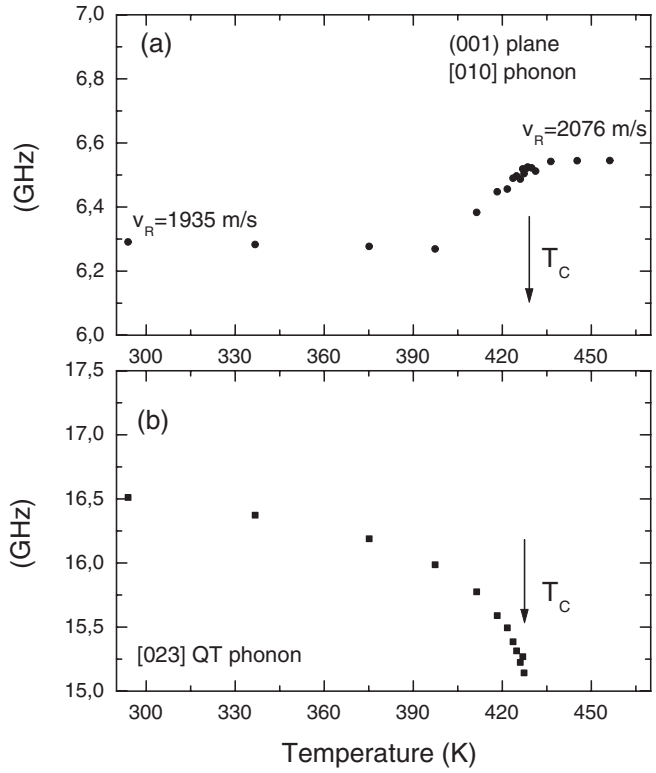

Figure 11. The result of simultaneous observation of surface (a) and bulk (b) phonons in β-GMO.

vation of these two types of phonons does not permit us to conclude that the bulk transition and the surface anomaly occur at different temperatures (see figure 11). However, it has been shown that the bulk transition occurs in a wider temperature range than the surface phonon anomaly.

We expect that it would be possible to explain the main controversy of our paper, namely, the unexpected difference between the calculated and experimental Rayleigh SAW results, if we were able to define exactly the real surface of the crystal.

4. Summary

Temperature dependences of all components of the β-GMO crystal elasticity tensor were determined. The greatest softening near the phase transition temperature was observed for the elastic constants c_{11}, c_{22} and c_{66}, whose values decreased by over 20%. The other components of the elasticity tensor did not show such significant anomalies. Small softening was observed for the constants c_{33}, while the c_{44} constant remained unchanged. The other non-diagonal components c_{12} and c_{13} obtained indirectly were also found to show anomalous changes at the phase transition. The temperature dependences of the non-diagonal components were significantly affected by the values of the diagonal ones, according to the formulae given in table 1.

The temperature dependences of the surface phonons calculated numerically by the iterative method proposed by Farnell and based on the dependences for the bulk phonons for the β-GMO crystal reveal surface phonon softening at the phase transition. In the experimental system applied when the angle of light incidence was 60°, a surface layer of about 300 nm could be observed. The experimentally determined temperature behaviour of the velocity of the surface phonon propagation in this layer was different from that expected on the basis of the numerical calculations. The Brillouin shift of the surface phonons observed did not show the expected decrease at the phase transition. Only a few per cent increase in the surface phonon velocity was found to accompany the phase transition.

The question is what the reasons are for such significant differences in the temperature dependences of the surface phonons determined in experiment and by the numerical iterative method. The iterative method based on the values of the components of the bulk elasticity tensor as the initial data assumes the lack of significant differences in the crystal structure in the bulk and on the surface. In this method the surface mode is realized in the ideal semispace of the crystal. Therefore, the differences in the temperature dependences of the surface phonon velocity obtained in experiment and from the calculations can be explained by the fact that the structure of the crystal surface is not an ideal reflection of its bulk structure. Because of the breaking up of the crystalline bonds and delamination of the cells on the surface obtained as a result of mechanical cut-off of the bulk crystal a new crystalline structure appears. As a consequence of displacements of some atoms from the equilibrium positions some new lattice planes appear. The above processes are inevitable on reconstruction of the real surface of the crystalline material [24].

The results of this study allow a conclusion that the phase transition occurs at the same temperature in the surface layer about 300 nm deep and in the bulk of the β-GMO crystal. However, the anomalous behaviour of the bulk phonons accompanying the phase transition occurs over a wider temperature range than that of surface phonons.

In the ferroelastic phase transition taking place in the crystal β-GMO at 430 K the aluminium film deposited on the crystal surface responds to the stress in the substrate. The change in the substrate symmetry and in the interatomic distances taking place at that temperature may lead to delamination, cracking of the aluminium film or even the loss of contact between the substrate and the film. Changes of this type would lead to loss of repeatability. As our measurements were repeated a few times and the results showed a significant repeatability we believe that the aluminium film deposited does not undergo substantial changes that would affect the surface effects observed. Of course this metal film is a certain load of the substrate

surface. In the Brillouin surface spectroscopy the effective thickness of the layer that we are able to study varies in the range from about 270 nm to about 900 nm. However, the spectrum obtained should be regarded as averaged over the range. Assuming that the mechanical processing of the samples, deposition of the aluminium film and the effect of the substrate loading affect the substrate to the thickness of about a few tens of nanometres, it is still a reasonable approximation because the thickness of the layer penetrated by the laser radiation is about 300 nm so the information obtained is dominated by the effect of the undisturbed layer. An increase in the thickness of the near surface layer studied by 100 nm (300 nm–400 nm–500 nm) changes the character of the anomaly observed into that of an increasingly soft bulk mode. If the destroyed near-surface layer had a thickness of a few micrometres, no such behaviour of the surface phonons would have been observed. We have observed an effect of this type for the crystal $LiCsSO_4$ [25] and the study of this effect in β-GMO is underway.

References

[1] Beghi M G, Bottani C E, Ghislotti G, Amato G and Boarino L 1997 *Thin Solid Films* **297** 110
[2] Every A G 2002 *Meas. Sci. Technol.* **13** R21
[3] Pang W, Every A G, Comics J D, Stoddart P R and Zhang X 1999 *J. Appl. Phys.* **86** 331
[4] Sussner H, Pelous J, Schmidt M and Vacher R 1980 *Solid State Commun.* **36** 123
[5] Hillebrands B, Mock R, Guntherodt G, Bechthold P S and Herres N 1986 *Solid State Commun.* **60** 649
[6] Lefeuvre O, Pang W, Zinin P, Comins J D, Every A G, Briggs G A D, Zeller B D and Thompson G E 1999 *Thin Solid Films* **350** 53
[7] Sandercook J R 1982 *Trends in Brillouin Scattering* (*Topics in Applied Physics* vol 5) (Berlin: Springer)
[8] Toledano J C and Toledano P 1987 *The Landau Theory of Phase Transition* (Singapore: Word Scientific)
[9] Aizu K 1969 *J. Phys. Soc. Japan* **27** 387
[10] Dvorak V 1971 *Phys. Status Solidi* b **46** 763
[11] Höchli U T 1972 *Phys. Rev.* B **6** 1814
[12] Ullman F G, Ganguly B N and Hardy J R 1971 *Ferroelectrics* **2** 303
[13] Busch M, Toledano J C and Torres J 1974 *Opt. Commun.* **10** 273
[14] Itoh S and Nakamura T 1973 *Phys. Lett.* A **44** 461
[15] Luspin Y and Hauret G 1976 *Ferroelectrics* **13** 347
[16] Mroz B and Mielcarek S 2001 *J. Phys. D: Appl. Phys.* **34** 395
[17] Kumada A 1972 *Ferroelectrics* **3** 115
[18] Vacher R and Boyer L 1972 *Phys. Rev.* B **6** 639
[19] Farnel C W 1972 *Physical Acoustic* vol 9 (New York: Academic)
[20] Stoddart P R, Crowhurst J C, Every A G and Comins J D 1998 *J. Opt. Soc. Am.* B **15** 2481
[21] Cummins H Z and Schoen P E 1972 *Laser Handboock* (Amsterdam: North-Holland)
[22] Fedorov F I 1968 *Theory of Elastic Waves in Crystals* (New York: Plenum)
[23] Bjerkan L and Fossheim K 1977 *Solid State Commun.* **21** 1147
[24] Unertl W N 1996 *Physical Structure* vol 1 (Amsterdam: Elsevier)
[25] Trzaskowska A, Mielcarek S and Mroz B 2004 *Ferroelectrics* **303** 145